Journal of Nuclear Materials 390–391 (2009) 886–890

Contents lists available at ScienceDirect

Journal of Nuclear Materials

journal homepage: www.elsevier.com/locate/jnucmat

The effects of high fluence mixed-species (deuterium, helium, beryllium) plasma interactions with tungsten

M.J. Baldwin [a,*], R.P. Doerner [a], D. Nishijima [a], K. Tokunaga [b], Y. Ueda [c]

[a] Center for Energy Research, University of California at San Diego, San Diego, CA 92093, USA
[b] Research Institute for Applied Mechanics, Kyushu University, Fukuoka, Japan
[c] Graduate School of Engineering, Osaka University, Osaka, Japan

ARTICLE INFO

PACS:
52.40.Hf

ABSTRACT

W targets are exposed to D_2–Be, He, D_2–He and D_2–Be–He plasmas in the linear-plasma-device PISCES-B to simulate the conditions expected at W strike-points in an ITER all W metal divertor scenario. In D_2–Be and He plasmas, target temperatures in the range 1070–1320 K lead to surface layers of Be–W alloy or nano-structured W morphology, respectively, but below 900 K, neither types of layer are found to form. Both processes have kinetics reminiscent of diffusion. Alloying kinetics are optimal when surface Be availability is maximized through the formation of a deposited Be over-layer. Nano-structured layer growth at 1120 K is most rapid for incident He ion fluxes above 7×10^{21} $m^{-2}s^{-1}$. In D_2–0.1He plasmas, a mixture relevant to divertor exhaust, small Be or C fractions can significantly reduce nano-structure growth in favor of the formation of a mixed material Be–W alloy or C layer.

1. Introduction

W is considered the leading first-wall candidate material for next generation fusion reactors because of its ability to withstand intense heat loads, high operation temperatures and intense particle loads. Only graphite is better in comparison, but current philosophy is to limit or avoid altogether the use of carbon in next generation devices because of well known issues associated with neutron damage and tritium accumulation. The removal of carbon from the ITER design is referred to as the ITER 'all metal' divertor option; in essence, castellated W strike-points would replace the current graphite design. In the current ITER design, W surfaces (liner and dome) are designed operate at temperatures below 900 K [1] in contact with the weaker edge plasma. In contrast, an 'all metal' divertor would operate with high-temperature W strike-points, >1000 K, that are in contact with the full diverted plasma exhaust of ionized D, T, He and impurity Be species eroded from the first-wall. A similar scenario (but without Be) is also presented with the concept of a full W metal DEMO reactor.

The desire to operate W surfaces in increased temperature and mixed-species plasma regimes reveals a wide-ranging PMI parameter space that is essentially unexplored. In recent years, the UCSD PISCES program and collaborators have actively explored the use of W above 1000 K in plasma regimes that support ITER and advanced reactor PMI development needs. Experiments involving W target operation in plasmas of mixed-species of, D_2–Be, pure He and D_2–He have been undertaken with the aim of examining surface properties, erosion, and hydrogen isotope retention, subsequent to plasma exposure. This paper reports on the first of these issues; the effects of these plasmas on material surface properties.

2. Experiments

Polished W targets, 25 mm in diameter and 1 mm thick, were exposed to various plasmas in the UCSD PISCES-B divertor plasma simulator [2]. The effects of D_2 plasmas with Be injection, D_2 plasmas with He admixtures, D_2 plasmas with He admixtures and Be injection, and pure He plasmas were explored and compared. Typically, PISCES-B plasmas in D_2 are relevant to the edge in a fusion device, $n_e \sim 10^{18}$–10^{19} m^{-3}, and, $T_e \sim 6$–12 eV, as measured by Langmuir probe. Trace amounts of Be or He were added to the plasma, where necessary, to examine the effects that these species may produce on W surfaces. Be is incorporated into the plasma using a neutral Be atom source [3], and He through gas admixture. Both Be and He ion fractions in the plasma are measured using absolutely calibrated optical emission spectroscopy [3,4]. During plasma exposure the target temperature, T_s, is kept fixed and a bias potential applied to facilitate bombardment of the target with energetic ions. The energy of impacting ions is estimated from the target bias, $\langle E_{ions} \rangle \approx V_{bias} - kT_e$ [5]. Subsequent to plasma exposure, W targets are analyzed using scanning electron microscopy (SEM) to examine changes in surface morphology, and wavelength dispersive X-ray spectroscopy (WDS) to determine surface composition.

* Corresponding author. Tel.: +1 858 534 1655.
E-mail address: mbaldwin@ferp.ucsd.edu (M.J. Baldwin).

0022-3115/$ - see front matter © 2009 Elsevier B.V. All rights reserved.
doi:10.1016/j.jnucmat.2009.01.247

3. Results and discussion

3.1. W exposed to D_2 plasmas with Be injection

In ITER, the divertor surfaces could potentially see fluxes of incident Be as high as $\sim 3 \times 10^{21}$–3×10^{22} $m^{-2}s^{-1}$ [6]. For plasma conditions that favor the net build-up of Be deposits, concern arises over the alloying of deposits with the W surface because the Be–W matrix can support equilibrium molten phases at temperatures significantly below the W melting point (3695 K). Be uptake into the W above ~5 at.%, but below 67% results in the formation of molten phase precipitates above ~2370 K . With further Be uptake the situation worsens; the stable alloy stoichiometries of Be_2W, $Be_{12}W$ and $Be_{22}W$ precipitate and these are molten at even lower temperatures; ~2520 K, ~1780 K, and ~1600 K, respectively [7].

In the current ITER design the W liner and dome are specified to operate below ~900 K. In this range, Be–W alloying is not expected to be a serious concern. Not only have several studies shown that the reaction of Be deposits on W proceeds too slowly to cause alarm [8,9], but the temperature is too low to support any molten phase. In fact, in this temperature range, where W blistering is known be problematic [10], PISCES-B experiments repeatedly show that a small amount of Be ($f_{Be} \sim 0.0005$) in the plasma suppresses the formation of blisters. W targets exposed at 700 K, to ionized deuterium fluences up to 10^{27} m^{-2}, show the absence of blistering in favor of the formation of a thick (~several micro meter) Be layer on targets with no applied bias, and a thin (~10–20 nm) layer of Be–W alloy for targets with ion bombardment in the energy range, 35–75 eV. Control targets, exposed at 700 K to D_2 plasma, but without Be injection, reveal abundant blistering.

Experiments conducted above 1000 K, to simulate W strike-points in an ITER 'all metal' divertor, tell a very different story. All PISCES-B W targets exposed above 1000 K to D_2 plasma with Be injection show evidence of the formation of a Be–W alloy surface layer, to some degree. The observed degree of alloying depends critically on the availability of surface Be. However, while the alloy reaction rate is found to increase with surface temperature [9], Be removal mechanisms such as physical erosion and evaporation at high-temperature can work to limit this availability in a PMI situation. A selection of D_2–Be plasma exposed W targets demonstrates this in Fig. 1. In Fig. 1(a), a Be_{12} W layer ~0.3 μm thick is found at the interface between the W surface and a ~5 μm thick layer of Be surface deposits. The combination of an exposure temperature of 1070 K (low Be evaporation) and no applied target bias (low Be erosion) gives PMI conditions that maximize the surface Be availability for alloying. For the similarly plasma-exposed W target of Fig. 1(b), Be availability is deliberately reduced by the application of a target bias and associated ion bombardment at ~60 eV. Consequently, there is no apparent layer of deposited Be, as in Fig. 1(a). The absence of Be deposits is due to removal by sputtering. The reduction in surface Be results in only small ~0.3 μm high nucleation zones of ~Be_{12} W alloy distributed over a W rich surface (Cross-sectional analysis did not reveal Be below the surface). Higher surface temperature produces a similar effect as shown in Fig. 1(c). This W target had a higher exposure temperature of 1320 K (Be evaporates) and no applied bias (low Be erosion). On examination this target surface showed little, or no, evidence of an alloy layer. The rapid evaporation of deposited Be, leading to low Be availability, acted to inhibit the formation of Be deposits and the alloy reaction, and, in spite of increased mobility for Be in the bulk, cross-sectional analysis revealed little evidence for any Be below the surface. These results are further explored in Section 3.4.

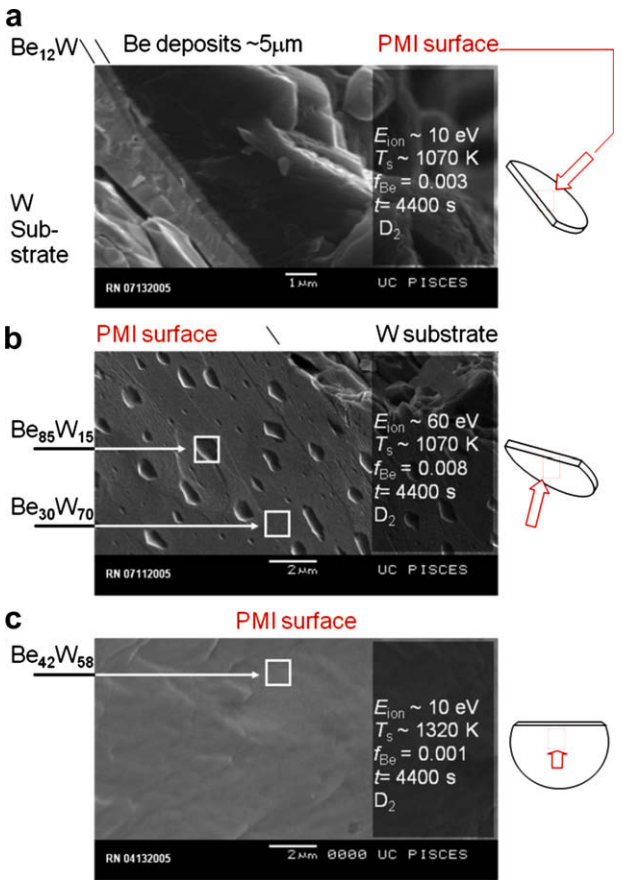

Fig. 1. Cross-sectional SEM images of W targets exposed to D_2 plasmas with Be injection. The plasma properties were $n_e = 3 \times 10^{18}$ m^{-3} and $T_e \sim 6$–8 eV, $\Gamma_{D^+} = 2$–3×10^{22} $m^{-2}s^{-1}$. Compositional data is provided by standardized WDS analysis at 5 kV. Symbols to the right indicate target cross-section orientation in SEM field of view and PMI surface.

3.2. W exposed to pure He plasma

Many studies have identified deleterious effects induced by helium plasmas on high-temperature exposed tungsten surfaces for incident He ion energies below the sputter threshold. In a few instances, He blistering is observed at moderate temperature below 800 K [11], but more serious effects such as the formation of pits, holes and bubbles occur at high-temperature, above 1600 K [12–14]. The accumulation of He in defects and vacancies [15,16] is believed to be responsible for these effects but the precise mechanisms are not well understood.

In the temperature range 1070–1600 K, particularly relevant to the ITER 'all metal' scenario, a surface layer consisting of a conglomerate of amorphous W nano-rod like structures is found to form under exposure to helium plasma [17,18] in the divertor plasma simulators NAGDIS-II and PISCES-B. Nano-rod dimensions can be up to a micron in length but have characteristic widths of the order of only 10–50 nm. X-ray micro-analysis, which is insensitive to He, reveals the nano-structured layer to be consistent with pure W. The nano-structured layer is visually black and apparent to the eye after only 200–400 s of exposure to He plasma in PISCES-B. Nano-structured layers are found to form readily at 1070 K, but not at a reduced temperature of 900 K, even after 3600 s of He plasma exposure. Interestingly, individual nano-structures contain nanometer scale bubbles or voids [19]. Fig. 2 shows an example of a nano-structured layer growing from the W bulk on a single crystal W target that was exposed to pure He plasma at 1120 K for 3600 s. Only a fraction of the ~2.0 μm thick layer is shown.

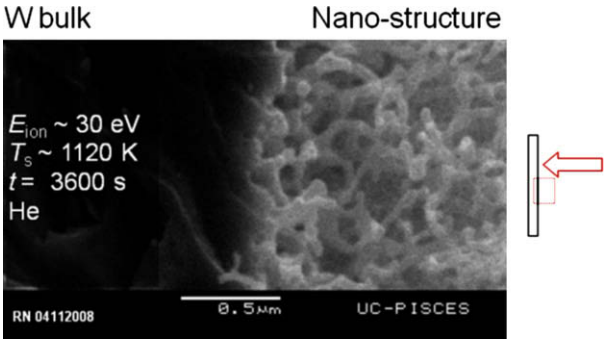

Fig. 2. Cross-sectional SEM micrograph of a single crystal W target that was exposed at 1120 K to pure He plasma for 3600 s. The plasma properties were $n_e = 5 \times 10^{18}$ m^{-3} and $T_e \sim 10$ eV, $\Gamma_{He^+} = 6 \times 10^{22}$ m^{-2}s^{-1}. Symbols to the right indicate target cross-section orientation in SEM field of view and PMI surface.

Evidently, the increased surface area, and fragility of these interconnected nano-structured layers raises new concerns for the use of W as a fusion reactor plasma-facing material. Surface thermal properties, fuel retention, and the formation of tungsten nano-dust are issues that require further scientific investigation.

In Fig. 3 growth of the nano-structured layer with plasma exposure time is demonstrated. SEM cross-sections of W targets exposed at 1120 K to pure He plasmas for durations of 2000, 9000, and 2.2 × 10^4 s are shown. For the longest exposure time explored, a nano-structured layer in excess of 5 μm thick is observed. Collectively, the kinetics of layer growth follows the kinetics of a diffusive process. Fig. 4(a) shows nano-structured layer thickness data, taken from images such as in Fig. 3, as a function of the square root of the plasma exposure time, for exposures conducted at 1120 K. The set of data demonstrates agreement with fitted $t^{1/2}$ dependence. The nano-structured layer growth is therefore governed by a diffusive like mechanism. In Fig. 4(a) the corresponding coefficient of diffusion would be $D_{1120\ K} = 6.8 \pm 0.3 \times 10^{-16}$ m^{2}s^{-1}, but it is yet uncertain what precise mechanism, or combined mechanisms, that this diffusion rate corresponds with. Presently, it is speculated [19] that the production of thermal vacancies, and diffusion of He in the W nano-structure matrix, play a convolved role. It is also interesting to note that the straight line fit is not consistent with a zero intercept. The $t^{1/2}$ axial intercept corresponding to $t \sim 40$ s may be an indication of a short incubation, or saturation time that precedes nano-structuring. Whatever the mechanisms involved, the continual surface disintegration of W,

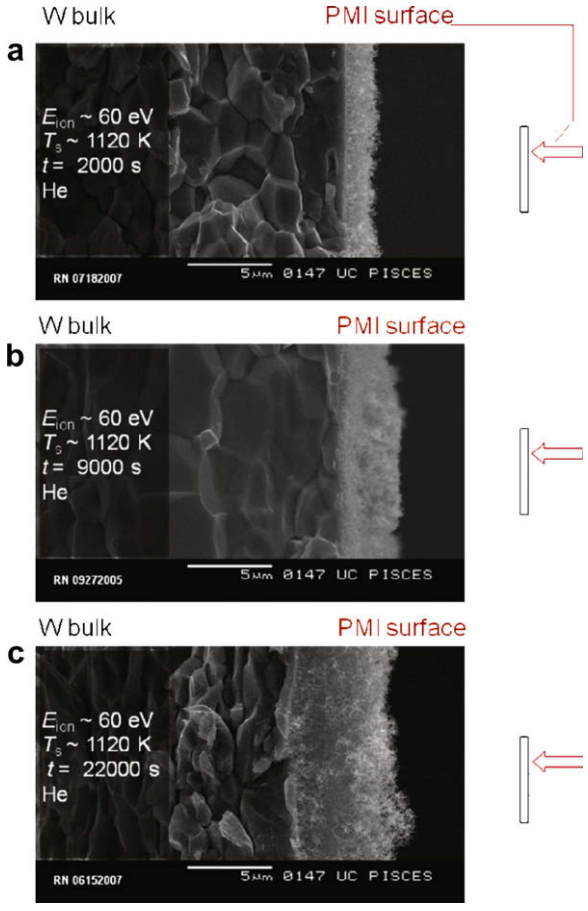

Fig. 3. Cross-sectional SEM images of W targets exposed to pure He plasma at 1120 K for various exposures times. The plasma properties were $n_e = 4 \times 10^{18}$ m^{-3} and $T_e \sim 6$–8 eV, $\Gamma_{He^+} = 4$–6×10^{22} m^{-2}s^{-1}. Symbols to the right indicate target cross-section orientation in SEM field of view and PMI surface.

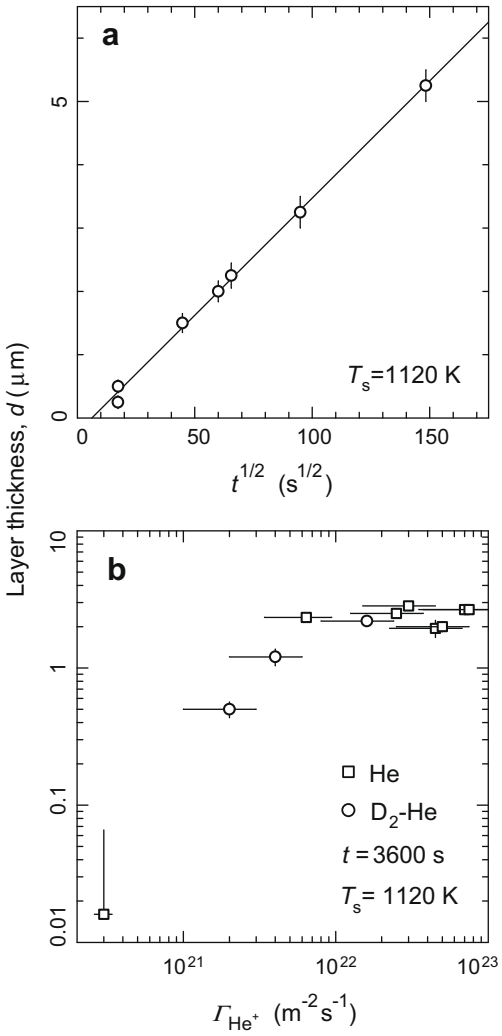

Fig. 4. (a) Plot of W nano-structured layer thicknesses against the square root of He plasma exposure time. The target temperature was 1120 K. If the simple one dimensional growth law, $d = (2Dt)^{1/2}$ is assumed, a straight line fit corresponds to a diffusional growth process characterized by a diffusion coefficient of $D_{1120\ K} = 6.8 \pm 0.3 \times 10^{-16}$ m^{2}s^{-1}. (b) Plot of W nano-structured layer thicknesses after 3600 s of exposure to He plasma, against plasma-surface He ion flux. All targets were exposed at a temperature of 1120 K. Data are shown for both pure He and D_2–He plasmas.

in this way, may lead to a source of plasma induced W erosion that has not been previously considered.

3.3. W exposed to D_2–He mixture plasmas

In the more realistic reactor PMI scenario, high-temperature exposed W will not be subject to pure He plasma. The He level in the ITER reactor exhaust for example is not expected to exceed, $f_{He} \sim 0.1$ [20], with the balance being largely hydrogen isotopes. To explore the effects of Section 3.2 in this situation, W targets were exposed at 1120 K, for durations of 3600 s to various D_2–He mixture plasmas. Cross-sectional SEM analysis, as in Fig. 3, revealed the same surface modification by the growth of nano-structures, but with reduced layer growth kinetics compared to that described in Fig. 4(a) for pure He. Layer growth is diminished for low concentrations of plasma He up to $f_{He} \sim 0.3$ compared to pure He plasma exposure under similar conditions. A trend emerges, however, when the growth of the nano-structured layer is plotted against the incident He ion flux. This is depicted in Fig. 4(b), which shows nano-structured layer thicknesses for many targets exposed in both D_2–He mixture and pure He discharges. The plot displays two regions of interest. For plasmas that have low bombardment fluxes of less than $\sim 7 \times 10^{21}$ He ions $m^{-2}s^{-1}$, the growth rate of the nano-structured layer, and hence diffusive kinetics, are influenced by the magnitude of the He ion flux. Above $\sim 7 \times 10^{21}$ He ions $m^{-2}s^{-1}$ the rate of growth is independent of the He ion bombardment flux. In the D_2–He mixture cases, it is speculated that the presence of ionized deuterium is not responsible for any reduction in the nano-structured layer growth rate. Indeed, the lowest He ion flux plasma exposure was conducted in a separate rf plasma device in pure He plasma. This single point also fits the observed trend and collectively implies that the availability of diffusing He, or He saturation of the W surface, plays a strong role in producing the visible evidence of a growing nano-structured layer. This would indirectly further the idea [18] that nano-structures form through the action of a mechanism that traps He.

3.4. W in D_2–He with Be and C injection: mixed material or nanoscopic morphology

Considering the results of Section 3.3 the question arises about the influence of other impurity species since the divertor plasma in ITER is likely to contain a significant Be fraction. To explore this, additional W targets were exposed at 1150 K to D_2–0.1He admixture plasmas with Be injection, and CD_4 gas admixture. These results are shown in Fig. 5. Fig. 5(a) depicts the cross section of a control W target exposed to D_2–0.1He plasma for 4200 s. In this case, an applied bias provides an ion bombardment energy of ~60 eV. The plasma exposure produces a nano-structured layer of thickness ~0.4 μm. Although not shown, a similarly exposed target, but with Be injection, $f_{Be} \sim 0.001$, revealed a near identical nano-structured layer. In this case, Be availability was reduced by physical erosion, as in Fig. 1(b), and the morphology dominated by processes associated with He. A different story is apparent, however, when Be availability is increased. In Fig. 5(b) the ion energy is reduced to ~15 eV. In this case, a layer of Be–W alloy is formed and the effects associated with He are not apparent. CD_4 injection produces a similar effect at low energy ~15 eV. In Fig. 5(c), a small amount of carbon impurities in the plasma, $f_C < 0.001$, results in a thin ~0.2 μm thick layer of almost pure C that ultimately prevents nano-structures from forming.

Figs. 1 and 5 demonstrate how sensitive that PMI processes are to the composition of the near surface. At 60 eV, the stopping range for both D^+ and He^+ is under 30 nm in Be or C, so even this small amount in the form of a protective layer will have a great impact on the type of surface modification observed on a W surface.

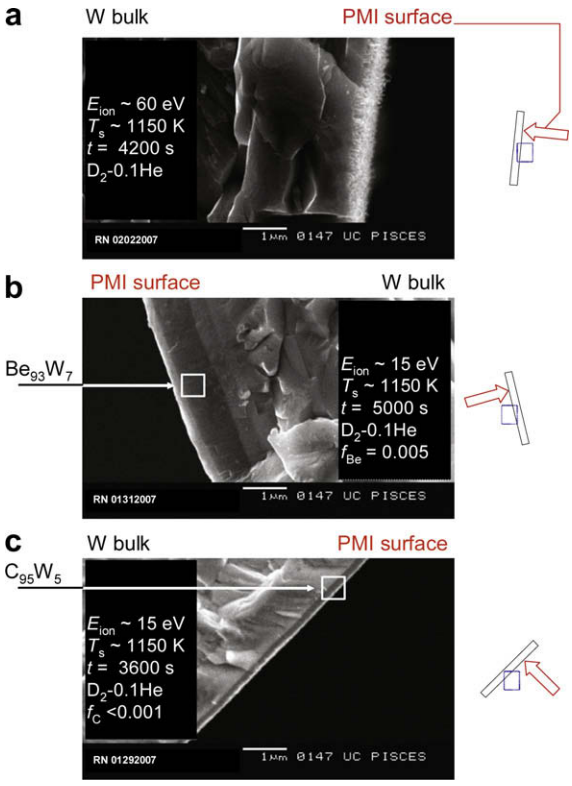

Fig. 5. Cross-sectional SEM images of W targets exposed to D_2–0.1He plasma at 1150 K. (a) D_2–0.1He, (b) D_2–0.1He with Be injection, (c) D_2–0.1He with CD_4 gas admixture. The plasma properties were $n_e = 2–3 \times 10^{18}$ m^{-3} and $T_e \sim 10–15$ eV, $\Gamma_{He^+} = 1–3 \times 10^{22}$ $m^{-2}s^{-1}$. Symbols to the right indicate target cross-section orientation in SEM field of view and PMI surface.

4. Summary and conclusions

W targets exposed to PISCES-B D_2 plasmas with Be injection in the temperature range 1070–1320 reveal the formation of Be–W alloy surfaces. Alloying kinetics are found to be optimal when Be availability at the surface is maximized through the formation of a layer of Be deposits. Reduced availability brought about by re-erosion and/or evaporation at high-temperature, is found to inhibit reaction kinetics in a PMI situation.

In He plasma, W exposed in the temperature range 1070–1320 K is found to develop a nano-structured surface layer consisting of nano-rod like structures. The growth of the thickness of the nano-structured layer is observed to have kinetics reminiscent of diffusion. The impact of W surface nano-structure morphology on fusion reactor performance is not fully clear. Such structures could potentially source high-Z dust, and have different properties of retention and thermal conduction compared to a planar W surface. As such, these issues alone warrant further scientific investigation.

In D_2–He mixture plasmas the presence of deuterium does not appear to have an influence on the formation of W nanoscopoic morphology. A reduced nano-structured layer growth rate in D_2–He mixture plasmas is more likely to be linked to the dilution of the impinging He ion flux rather than a plasma-materials effect. This suggests that nano-structures grow through the action of a mechanism that requires saturation of the W matrix with He.

In D_2–0.1He plasmas, a mixture relevant to divertor exhaust, small impurity fractions can have a significant impact on the observed morphology. Changes in W surface properties are found to favor the most dominant impurity; Be–W alloy formation in the case of Be impurities, and nanoscopic morphology in the case of He.

Finally, a few comments can be made concerning an ITER all metal divertor. The ITER liner and dome are expected to operate

below 900 K. In this temperature range, the growth of reacted Be–W alloy should not be severe [8,9] and deposited Be may actually alleviate potential problems caused by W blistering. The formation of nanoscopic morphology might also be negligible since this temperature range was not sufficient to produce a nano-structured surface in PISCES-B pure He plasmas.

On the other hand, W metal strike-points would operate >1000 K. Here Be–W alloying may give rise to low melting point precipitate phases if the availability of Be is high, as in locations that support net Be deposition. In locations where Be does not accumulate, the formation of He induced nanoscopic morphology is likely to occur. Thus, while the W liner and dome are seemingly likely to escape these effects, W strike-points are almost certain to encounter at least one or more of these higher temperature Be or He induced phenomena.

Acknowledgements

The authors acknowledge PISCES-B technical support, particularly T. Lynch, and the beryllium enclosure personnel. This work is supported by US–EU and US–Japan Collaborations on Mixed Materials and DOE Grant No. DE-FG02-07ER54912.

References

[1] G. Federici, P. Andrew, P. Barabaschi, et al., J. Nucl. Mater. 313–316 (2003) 11.
[2] Y. Hirooka, R.W. Conn, T. Sketchley, et al., J. Vac. Sci. Technol. A 8 (1990) 1790.
[3] R. Doerner, M.J. Baldwin, K. Schmid, Phys. Scr. T111 (2004) 75.
[4] D. Nishijima, R.P. Doerner, M.J. Baldwin, E.M. Hollmann, R.P. Seraydarian, Phys. Plasmas 14 (2007) 103509.
[5] B. LaBombard, R.W. Conn, Y. Hirooka, R. Lehmer, W.K. Leung, R.E. Nygren, Y. Ra, G. Tynan, K.S. Chung, J. Nucl. Mater. 162–164 (1) (1989) 314.
[6] K. Schmid, M.J. Baldwin, R.P. Doerner, A. Wiltner, Nucl. Fus. 44 (2004) 815.
[7] T.B. Massalski, H. Okamoto, P.R. Subramanian, L. Kacprzak, Binary Alloy Phase Diagrams, Version 1.0, 2nd Ed., ASM International, Materials Park, Ohio, 1996.
[8] Ch. Linsmeier, K. Ertl, J. Roth, A. Wiltner, K. Schmid, F. Kost, S.R. Bhattacharyya, M. Baldwin, R.P. Doerner, J. Nucl. Mater. 363–365 (2007) 1129.
[9] M.J. Baldwin, R.P. Doerner, D. Nishijima, D. Buchenauer, W.M. Clift, R.A. Causey, K. Schmid, J. Nucl. Mater. 363–365 (2007) 1179.
[10] K. Tokunaga, M.J. Baldwin, R.P. Doerner, N. Noda, Y. Kubota, N. Yoshida, T. Sogabe, T. Kato, B. Schedler, J. Nucl. Mater. 337–339 (2005) 887.
[11] S. Nagata, B. Tsuchiya, T. Sugawara, N. Ohtsu, T. Shikama, J. Nucl. Mater. 307–311 (2002) 1513.
[12] D. Nishijima, M.Y. Ye, N. Ohno, S. Takamura, J. Nucl. Mater. 313–316 (2003) 97.
[13] M.Y. Ye, H. Kanehara, S. Fukuta, N. Ohno, S. Takamura, J. Nucl. Mater. 313–316 (2003) 72.
[14] D. Nishijima, M.Y. Ye, N. Ohno, S. Takamura, J. Nucl. Mater. 329–333 (2004) 1029.
[15] R.N. Stuart, M.W. Guinan, R.J. Borg, Radiat. Eff. 30 (1976) 129.
[16] V.N. Chernikov, H. Trinkaus, P. Jung, H. Ullmaier, J. Nucl. Mater. 170 (1990) 31.
[17] S. Takamura, N. Ohno, D. Nishijima, S. Kajita, Plasma Fus. Res. 51 (2006) 1.
[18] M.J. Baldwin, R.P. Doerner, Nucl. Fus. 48 (3) (2008) 035001.
[19] N. Yoshida, H. Iwakiri, in: Proceedings of the 1st International Symposium and 1st Korea–Japan Workshop on Edge Plasma and Surface Component Interactions in Steady State Magnetic Fusion Devices, 20–22 May 2007, Toki, Japan.
[20] A. Kukushkin, ITER Report, [ITER_D_27TKC6], 2008.